Science Advances
AAAS

advances.sciencemag.org/cgi/content/full/6/21/eaay5098/DC1

Supplementary Materials for

Supercooled liquid sulfur maintained in three-dimensional current collector for high-performance Li-S batteries

Guangmin Zhou, Ankun Yang, Guoping Gao, Xiaoyun Yu, Jinwei Xu, Chenwei Liu, Yusheng Ye, Allen Pei, Yecun Wu, Yucan Peng, Yanxi Li, Zheng Liang, Kai Liu, Lin-Wang Wang, Yi Cui*

*Corresponding author. Email: yicui@stanford.edu

Published 22 May 2020, *Sci. Adv.* **6**, eaay5098 (2020)
DOI: 10.1126/sciadv.aay5098

The PDF file includes:

Other Supplementary Material for this manuscript includes the following:

(available at advances.sciencemag.org/cgi/content/full/6/21/eaay5098/DC1)

Supplementary Figures

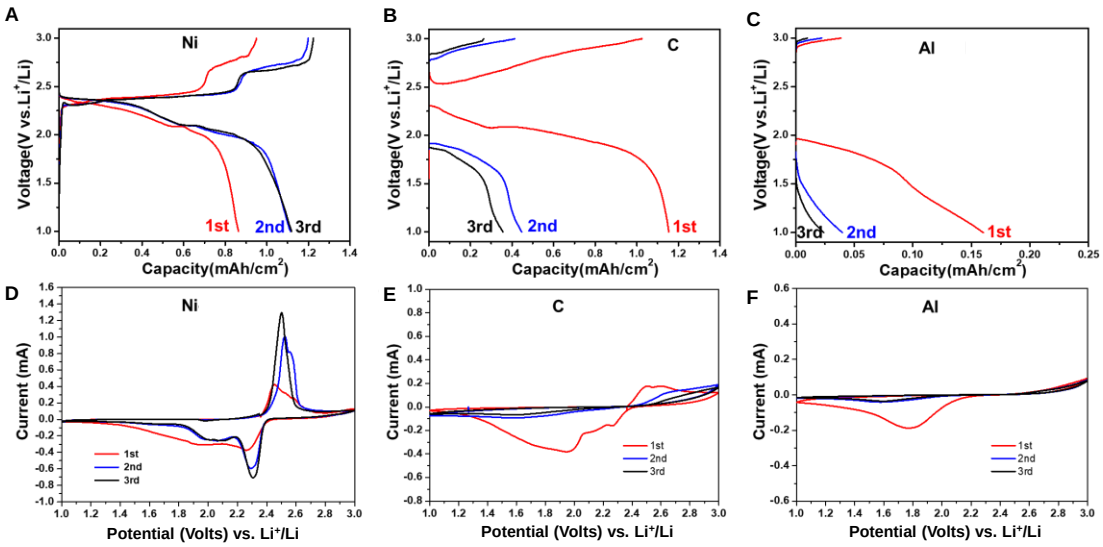

Figure S1. Charge/discharge voltage profiles of the (**A**) Ni, (**B**) C, and (**C**) Al electrodes at a current density of 0.05 mA cm^{-2}. CV curves of the (**D**) Ni, (**E**) C, and (**F**) Al electrodes at a scan rate of 0.1 mV s^{-1} for 3 cycles.

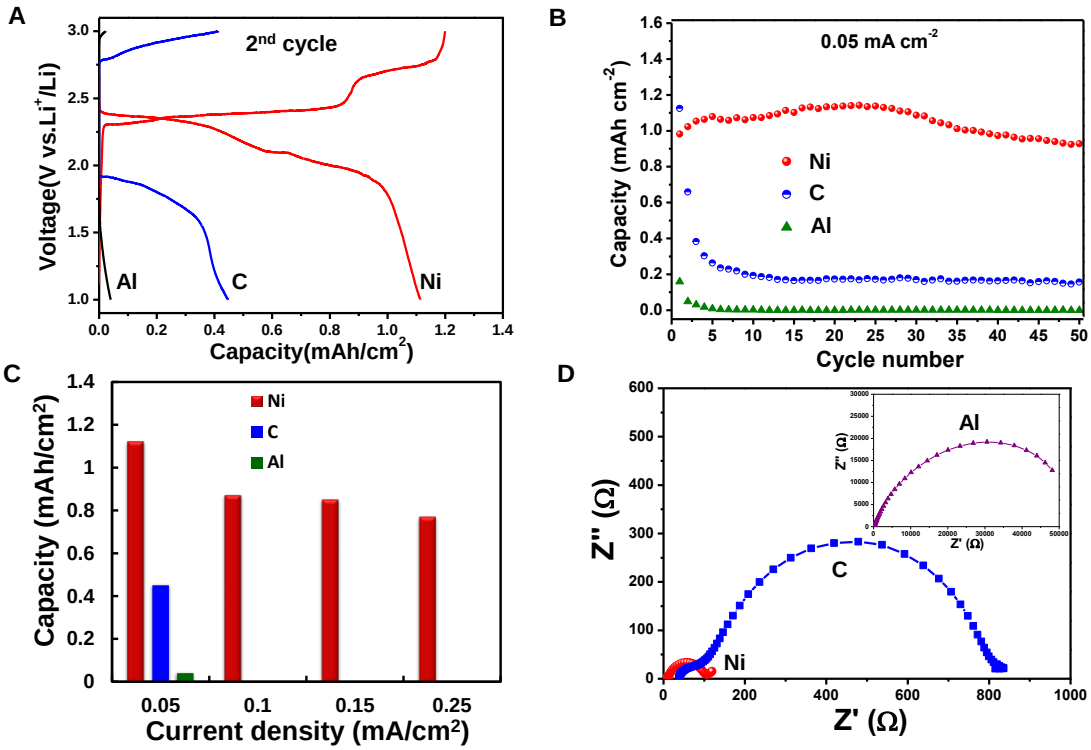

Figure S2. (**A**) Charge/discharge voltage profiles of the Ni, C, and Al electrodes at a current density of 0.05 mA cm^{-2}. (**B**) Cycling stability of the Ni, C, and Al electrodes

at a current density of 0.05 mA cm^{-2} for 50 cycles. (**C**) Comparison of the rate capacity of the Ni, C, and Al electrodes. (**D**) Nyquist plots of the Ni and C electrodes at open circuit before cycling at room temperature. Inset is the Nyquist plot of the Al electrode at open circuit before cycling at room temperature.

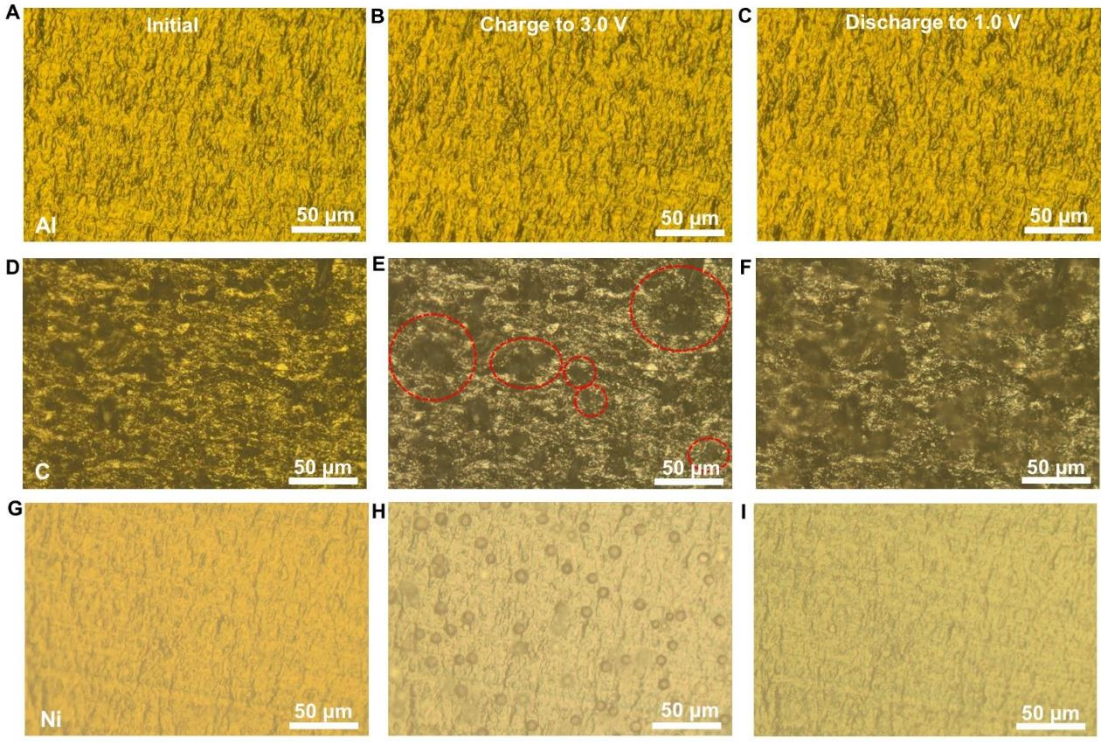

Figure S3. Optical images of the Al electrode in lithium polysulfide electrolyte (**A**) at initial state, (**B**) after charging to 3.0 V, and (**C**) after discharging to 1.0 V. Optical images of the C electrode in lithium polysulfide electrolyte (**D**) at initial state, (**E**) after charging to 3.0 V, and (**F**) after discharging to 1.0 V. Optical images of the Ni electrode in lithium polysulfide electrolyte (**G**) at initial state, (**H**) after charging to 3.0 V, and (**I**) after discharging to 1.0 V.

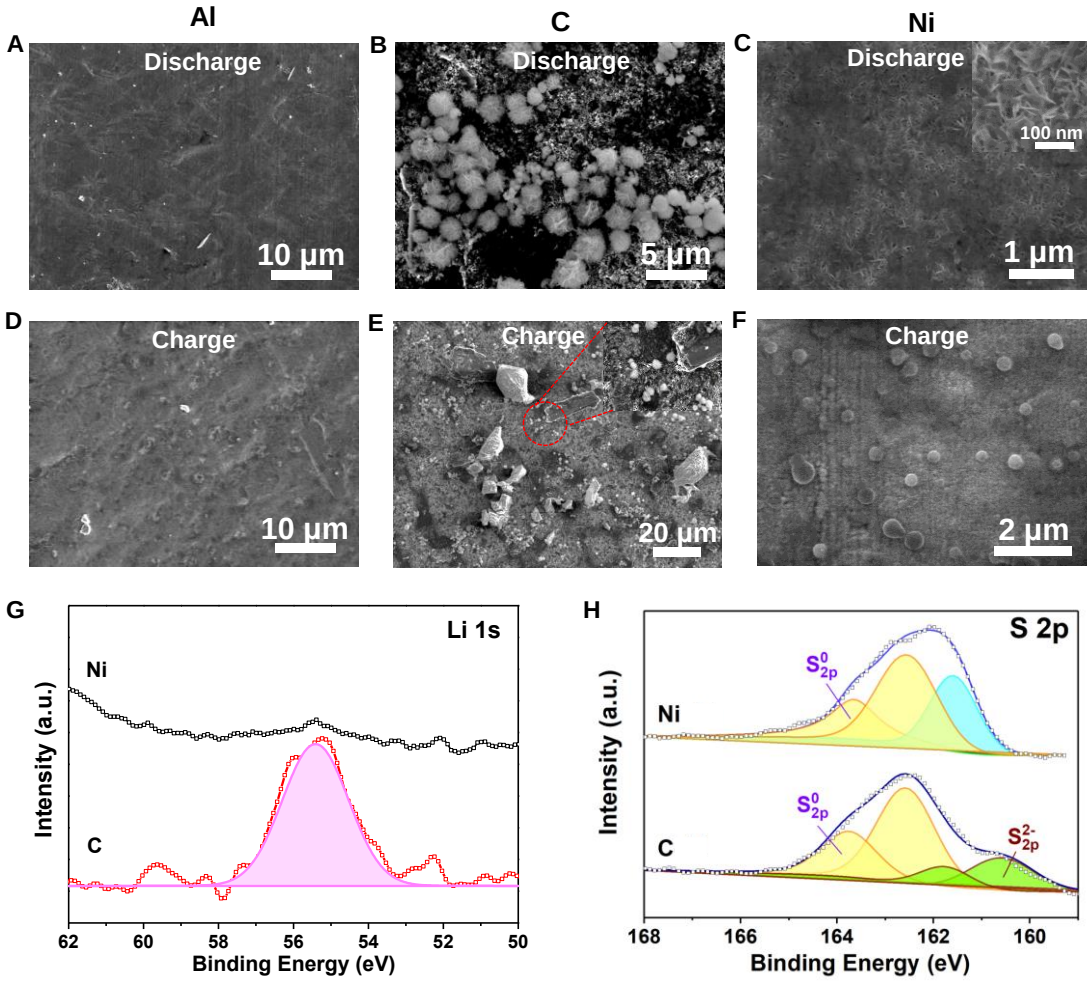

Figure S4. SEM images of the discharging products formed on the (**A**) Al, (**B**) C, and (**C**) Ni substrates. Inset in (**C**) is the magnified image. SEM images of the charging products formed on the (**D**) Al, (**E**) C, and (**F**) Ni substrates. Inset in (**E**) is the magnified area indicated by the red circle. (**G**) Li 1s XPS spectra of the Ni and C substrates. (**H**) S 2p XPS spectra of the Ni and C substrates.

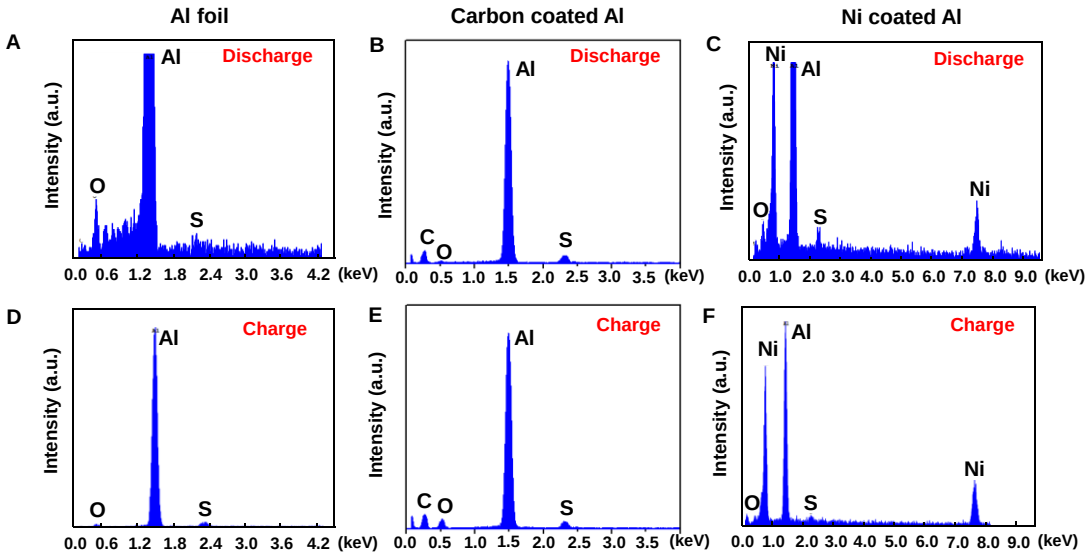

Figure S5. EDS of the discharging products formed on the (**A**) Al, (**B**) C, and (**C**) Ni substrates. EDS of the charging products formed on the (**D**) Al, (**E**) C, and (**F**) Ni substrates.

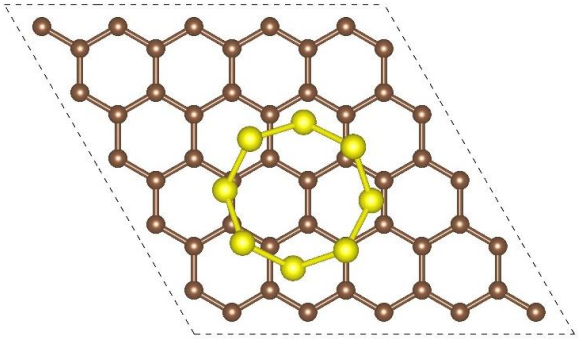

Figure S6. Adsorption energy and configuration of S_8 adsorbed on the basal plane of graphene.

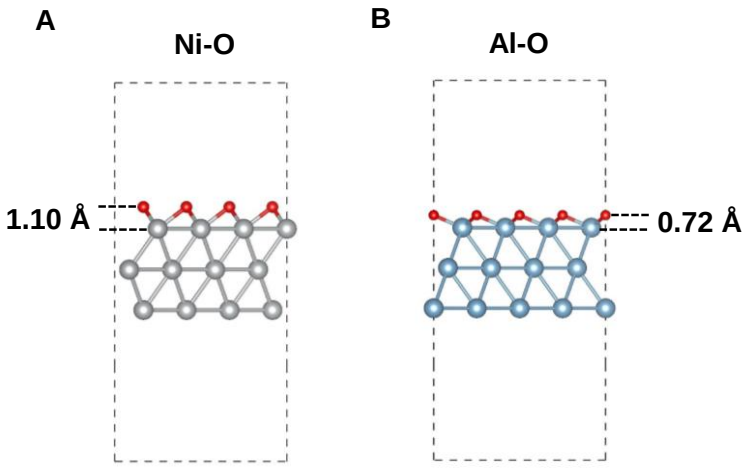

Figure S7. Configurations of the (**A**) Ni-O layer and (**B**) Al-O layer on the surface of nickel and aluminum, respectively.

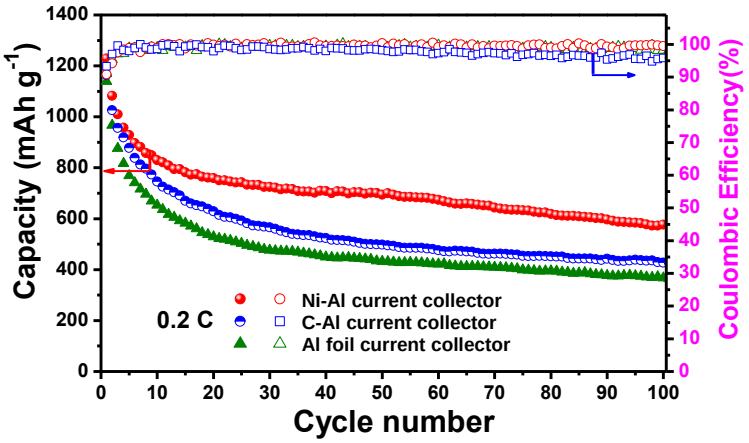

Figure S8. Cycling performance and Coulombic efficiency of the sulfur cathode coated on Ni, C and Al current collectors at 0.2 C for 100 cycles.

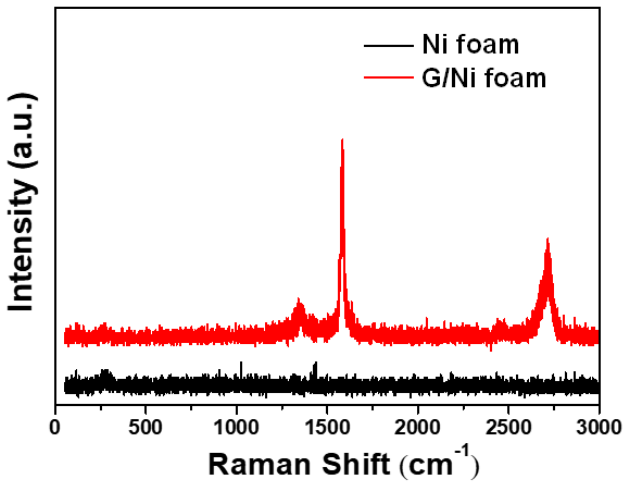

Figure S9. Raman spectra of Ni foam and G/Ni foam.

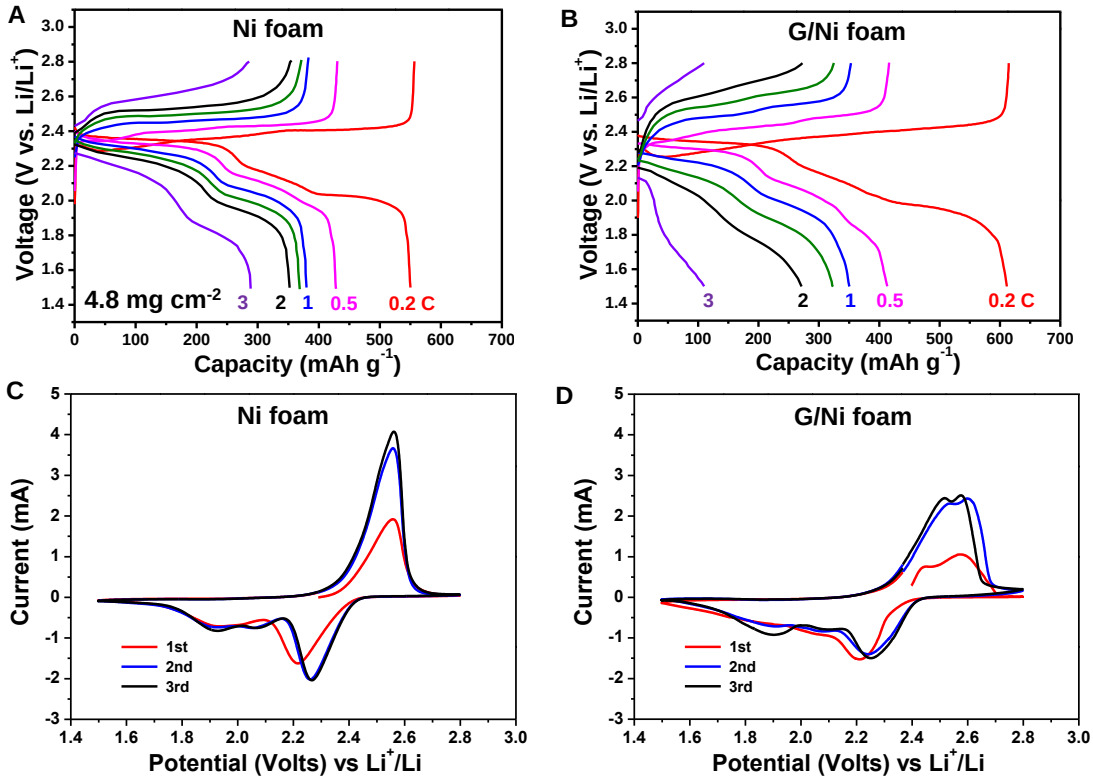

Figure S10. Charge/discharge voltage profiles of the (**A**) Ni foam and (**B**) G/Ni foam electrodes at different current densities. CV curves of the (**C**) Ni foam and (**D**) G/Ni foam electrodes at a scan rate of 0.1 mV s^{-1} for 3 cycles.

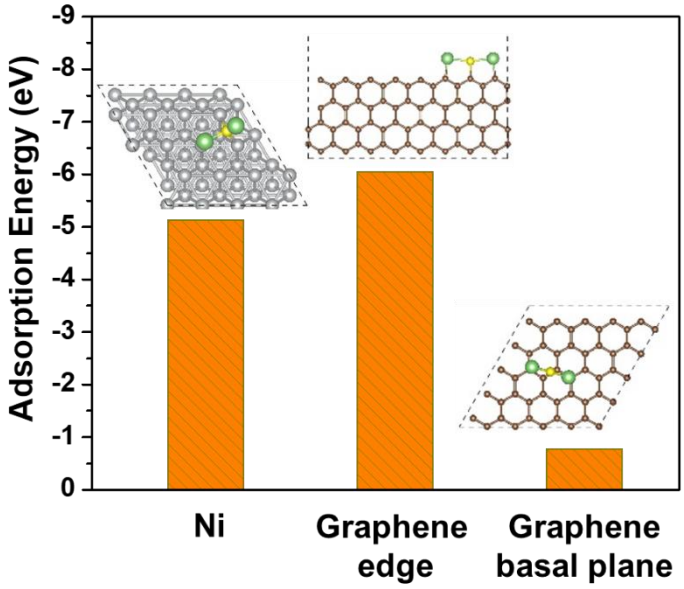

Figure S11. Adsorption energy and configurations of Li_2S adsorbed on the surface of Ni, graphene edge, and graphene basal plane.

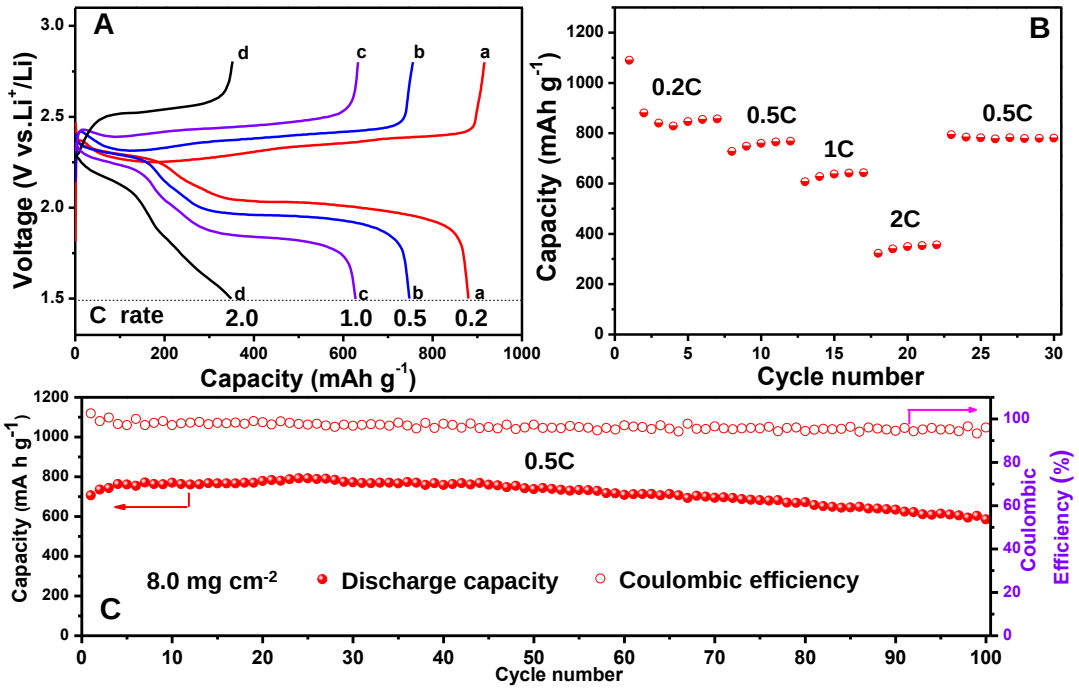

Figure S12. (**A**) Galvanostatic charge/discharge profiles of the nickel coated melamine foam electrode at various rates within a potential window of 1.5–2.8 V versus Li^+/Li^0. (**B**) Rate performance of the nickel coated melamine foam electrode at different current densities. (**C**) Cycling performance and Coulombic efficiency of the nickel coated melamine foam electrode at 0.5C rate for 100 cycles.

Supplementary Movie Captions

Supplementary Movie 1

Real time imaging for the solid sulfur crystal nucleation, growth, and dissolution processes on carbon electrode in lithium polysulfide electrolyte. The electrochemical cell was galvanostatically charged and discharged at 0.05 mA between 3.0 and 1.0 V. Play speed is 200x of the actual speed.

Supplementary Movie 2

Real time imaging for the liquid sulfur droplet nucleation, growth, and dissolution processes on Ni electrode in lithium polysulfide electrolyte. The electrochemical cell was galvanostatically charged and discharged at 0.05 mA between 3.0 and 1.0 V. Play speed is 25x of the actual speed.

Supplementary Movie 3

Real time imaging for the liquid sulfur droplet nucleation, growth, and dissolution processes on Ni foam electrode in lithium polysulfide electrolyte at a low magnification. The electrochemical cell was galvanostatically charged and discharged at 0.1 mA between 3.0 and 1.5 V. Play speed is 25x of the actual speed.

Supplementary Movie 4

Real time imaging for the liquid sulfur droplet nucleation, growth, and dissolution processes on Ni foam electrode in lithium polysulfide electrolyte at a high magnification. The electrochemical cell was galvanostatically charged and discharged at 0.1 mA between 3.0 and 1.5 V. Play speed is 25x of the actual speed.

Supplementary Movie 5

Real time imaging for the solid sulfur crystal nucleation, growth, and dissolution

processes on G/Ni foam electrode in lithium polysulfide electrolyte at a low magnification. The electrochemical cell was galvanostatically charged and discharged at 0.1 mA between 3.0 and 1.5 V. Play speed is 25x of the actual speed.

Supplementary Movie 6

Real time imaging for the solid sulfur crystal nucleation, growth, and dissolution processes on G/Ni foam electrode in lithium polysulfide electrolyte at a high magnification. The electrochemical cell was galvanostatically charged and discharged at 0.1 mA between 3.0 and 1.5 V. Play speed is 25x of the actual speed.

Supplementary Movie 7

Real time imaging for the liquid sulfur droplet nucleation and growth processes on Ni foam electrode in lithium polysulfide electrolyte. The electrochemical cell was constantly charged at 3.5 V. Play speed is 3x of the actual speed.

Supplementary Movie 8

Real time imaging for the solid sulfur crystal nucleation and growth processes on G/Ni foam electrode in lithium polysulfide electrolyte. The electrochemical cell was constantly charged at 3.5 V. Play speed is 3x of the actual speed.

Supplementary Movie 9

Real time imaging for the liquid sulfur droplet nucleation, growth, and dissolution processes on Ni coated melamine foam electrode in lithium polysulfide electrolyte. The electrochemical cell was galvanostatically charged and discharged at 0.08 mA between 3.0 and 1.5 V. Play speed is 25x of the actual speed.